LETTERS
PUBLISHED ONLINE: 25 APRIL 2010 | DOI: 10.1038/NNANO.2010.64
nature nanotechnology

Imaging and manipulating the spin direction of individual atoms

David Serrate[1†], Paolo Ferriani[1,2], Yasuo Yoshida[1], Saw-Wai Hla[1,3], Matthias Menzel[1], Kirsten von Bergmann[1], Stefan Heinze[1,2], Andre Kubetzka[1]* and Roland Wiesendanger[1]

Single magnetic atoms on surfaces are the smallest conceivable units for two-dimensional magnetic data storage. Previous experiments on such systems have investigated magnetization curves[1,2], the many-body Kondo effect[3,4] and magnetic excitations in quantum spin systems[5,6], but a stable magnetization has not yet been detected for an atom on a non-magnetic surface in the absence of a magnetic field. The spin direction of a single magnetic atom can be fixed by coupling it to an underlying magnetic substrate via the exchange interaction[7,8], but it is then difficult to differentiate between the magnetism of the atom and the surface. Here, we take advantage of the orbital symmetry of the spin-polarized density of states of single cobalt atoms to unambiguously determine their spin direction in real space using a combination of spin-resolved scanning tunnelling microscopy experiments and *ab initio* calculations. By laterally moving atoms on our non-collinear magnetic template[9], the spin direction can also be controlled while maintaining magnetic sensitivity, thereby providing an approach for constructing and characterizing artificial atomic-scale magnetic structures.

Magnetism of single atoms and nanostructures on surfaces is at the centre of solid-state research activities today. An ideal tool to investigate and build atomic-scale structures is the scanning tunnelling microscope (STM). Spin resolution has been demonstrated down to the atomic scale with magnetic tips[10] and atom manipulation has been performed with normal metallic tips[11]. Both are well-established techniques, but the combination of these two intriguing methods is still an experimental challenge. We have chosen the well-characterized atomic layer of manganese on W(110), which exhibits a spin spiral ground state[9], as our magnetic template for single cobalt atom adsorption. This template serves both as a reference to monitor the magnetization of the tip in our spin-polarized STM (SP-STM) measurements, and as a magnetic backbone to fix the spin of the adatoms by direct magnetic exchange interaction.

Figure 1 presents SP-STM constant-current images of single cobalt atoms adsorbed on Mn/W(110) obtained with an out-of-plane sensitive tip (see Methods). As sketched at the bottom of Fig. 1b, the manganese layer exhibits a robust cycloidal spin spiral induced by the Dzyaloshinskii–Moriya interaction, propagating along the $[1\bar{1}0]$ direction with an angle of $\sim 173^\circ$ between magnetic moments of adjacent atomic rows[9]. This spin spiral gives rise to periodic stripes on the manganese layer along the [001] direction (Fig. 1a,b), reflecting the almost antiferromagnetic order on the atomic scale. This apparent height contrast vanishes approximately every 6 nm along the $[1\bar{1}0]$ direction where the local manganese moments lie in the plane. Thus, the manganese layer not only has nearly opposite magnetic moments in neighbouring sites, but their orientation also varies gradually across the surface.

The adsorbed cobalt atoms reside in hollow sites (Fig. 2a) and have varying heights and shapes that strongly depend on their lateral position with respect to the underlying spin spiral (Fig. 1a,b). Three distinct cases are marked by boxes in Fig. 1a: the cobalt atoms appear higher when they are located on bright manganese atom rows (top) and lower on dark manganese rows (bottom). At sites where the spin spiral contrast vanishes (manganese moments are in plane), the cobalt atoms have an intermediate height (right). In addition to these height variations, the shape of the atoms appears to be different on bright and dark manganese rows. Figure 1c shows a magnified view of two cobalt atoms at positions where the manganese magnetic moments underneath point exactly upwards and downwards. Depending on which of these two possible orientations occurs, the cobalt atom appears either rotationally symmetric with its maximum height at its centre (left) or elongated with two lobes along the $[1\bar{1}0]$ direction and a central minimum (right). Because in equivalent images acquired with a non-magnetic tungsten tip all cobalt atoms appear identical (Supplementary Fig. S1), these variations in height and shape can only be of magnetic origin.

To explain such a dramatic change in appearance, we performed density functional theory calculations[12–14] (see Supplementary Methods S2) for this system in the geometry depicted in Fig. 2a. The calculations do not include the small deviation of $\sim 7^\circ$ from the collinear antiferromagnetic state, because our focus here is on the local electronic structure of the cobalt atoms. The calculated results reveal that the cobalt atom gains an energy of 145 meV by coupling ferromagnetically with the nearest manganese atoms (along the [001] direction) when compared to the antiferromagnetic case (Supplementary Fig. S3). In the limit of low bias voltage, only states close to the Fermi energy E_F contribute to the tunnel current. The spin polarization of the tip, $P_T = (n_T^{\uparrow} - n_T^{\downarrow})/(n_T^{\uparrow} + n_T^{\downarrow})$, and the angle θ between tip and local sample magnetization at position $\mathbf{r}$ determine whether the majority ($n^{\uparrow}$) or the minority states ($n^{\downarrow}$) of the sample (S) at E_F dominate the tunnel current $I(\mathbf{r})$, according to the following expression derived from the spin-polarized Tersoff–Hamann model[15]:

$$I(\mathbf{r}) \propto \left(1 + P_T \cos\theta(\mathbf{r})\right) n_S^{\uparrow}(\mathbf{r}) + \left(1 - P_T \cos\theta(\mathbf{r})\right) n_S^{\downarrow}(\mathbf{r}) \qquad (1)$$

The calculated local density of states (LDOS) for the cobalt atom in the vicinity of E_F displays a nearly circular shape for the majority channel, whereas the minority channel shows two lobes along the

[1]Institute of Applied Physics, University of Hamburg, Jungiusstrasse 11, D-20355 Hamburg, Germany, [2]Institute of Theoretical Physics and Astrophysics, Christian-Albrechts-Universität zu Kiel, Leibnizstraße 15, 24098 Kiel, Germany, [3]Nanoscale & Quantum Phenomena Institute, Physics & Astronomy Department, Ohio University, Athens, Ohio 45701, USA; †Present address: Instituto de Nanociencia de Aragón, University of Zaragoza, 50018, Spain.
*e-mail: kubetzka@physnet.uni-hamburg.de

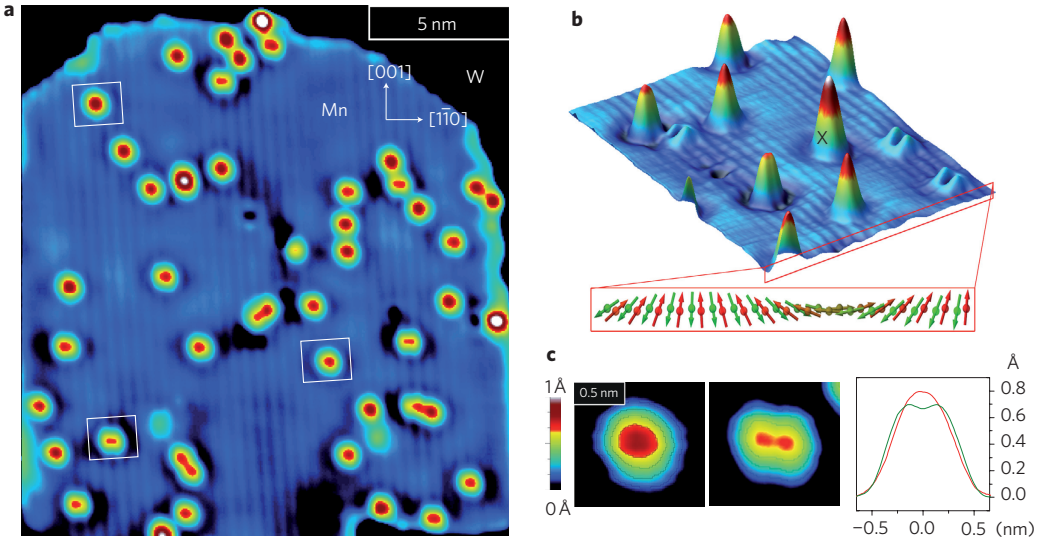

Figure 1 | SP-STM measurements of single cobalt atoms on one atomic layer of manganese on W(110), with a tip sensitive to the out-of-plane magnetization. a, Constant-current image ($U = -50$ mV, $I = 2$ nA). Periodic stripes along [001] indicate the magnetic contrast of adjacent atomic rows. The height and shape of the cobalt atoms depend critically on their position on the manganese spin spiral. **b**, Perspective view of a different sample area ($U = -10$ mV, $I = 2$ nA) and sketch of the manganese spin spiral (side view). A cobalt dimer is indicated by a black cross. **c**, Two particular cases (cobalt magnetic moment up and down) and the respective line profiles taken along the [1$\bar{1}$0] direction.

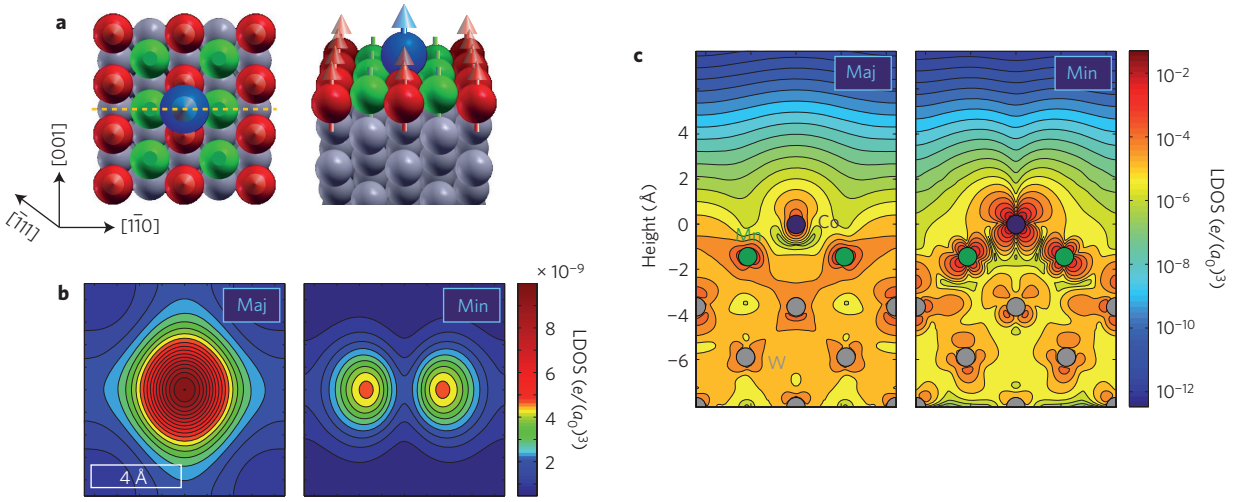

Figure 2 | Calculated spin-resolved local density of states of a cobalt atom on Mn/W(110). a, Top and perspective views of the unit cell used in the calculations. Red and green spheres represent manganese atoms with magnetization parallel and antiparallel to the cobalt atom (blue), respectively. **b**, LDOS in the energy interval between E_F and $E_F + 10$ meV for majority (maj) and minority (min) electrons in a plane parallel to the surface 5.2 Å above the cobalt atom (a_0 is the Bohr radius). **c**, As in **b** for a cross-section perpendicular to the surface along the dashed line in **a**. The positions of cobalt, manganese and tungsten atoms are marked for clarity.

[1$\bar{1}$0] direction with a minimum above the atom (Fig. 2b,c top and cross-sectional view), in excellent agreement with the SP-STM images in Fig. 1c. The different symmetries can be explained as follows. In the majority channel, the cobalt atom has a state composed of s, p_z and d_{z^2} orbitals, all of which are rotationally symmetric normal to the surface, with a maximum above the cobalt atom. For the minority channel, the LDOS is mainly given by a d_{xz} state, which exhibits a node at the cobalt atom centre and an overall reduced electron density (Supplementary Fig. S4). In an SP-STM experiment with $\theta = 0^\circ$, the majority channel ($n_S^{\uparrow}$) contributes predominantly to the tunnel current, but at $\theta = 180^\circ$ the contribution of $n_S^{\uparrow}$ is sufficiently suppressed and the d_{xz} character of $n_S^{\downarrow}$ becomes visible. For a spin-averaging tungsten tip ($P_T = 0$), $n_S^{\uparrow}$ dominates the vacuum LDOS and the d_{xz} orbital remains hidden (Supplementary Fig. S1).

As a function of lateral position, the spin of the cobalt atoms can be set to any direction that is available on the manganese spin spiral, which can be viewed as a process of writing information. Figure 3 shows a sequence of SP-STM images in which cobalt atoms were repositioned to an adjacent lattice site (see Methods), thereby practically inverting their spin direction. Initially, both cobalt atoms have a dominant majority component (Fig. 3a). Displacement of the left atom by one site along [$\bar{1}$11] switches its spin direction due to exchange coupling within the new lattice site and, as a consequence, the minority channel becomes dominant, giving rise to an elongated shape and lower apparent height (Fig. 3b). Between Fig. 3b and c the right atom has been moved one site along [1$\bar{1}\,\bar{1}$], and the minority channel is now dominant for both atoms.

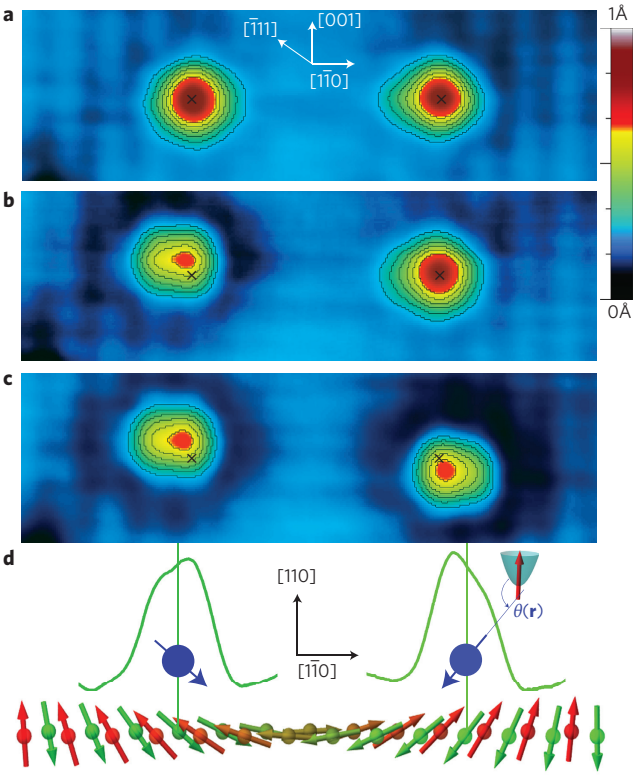

Figure 3 | SP-STM images showing cobalt atoms changing symmetry when moved to adjacent sites. Sequence of constant-current images ($U = +10$ mV, $I = 1$ nA): **a**, Starting configuration with black crosses as position markers. **b**, The left atom has been moved one site to the upper left. **c**, The right atom has been moved one site to the lower right. In the process, the spin directions have been changed by ~173° due to exchange coupling within the new adsorption sites. **d**, Line profiles across the centres of the atoms along [1$\bar{1}$0] in **c**, and sketch of the manganese spin spiral (side view).

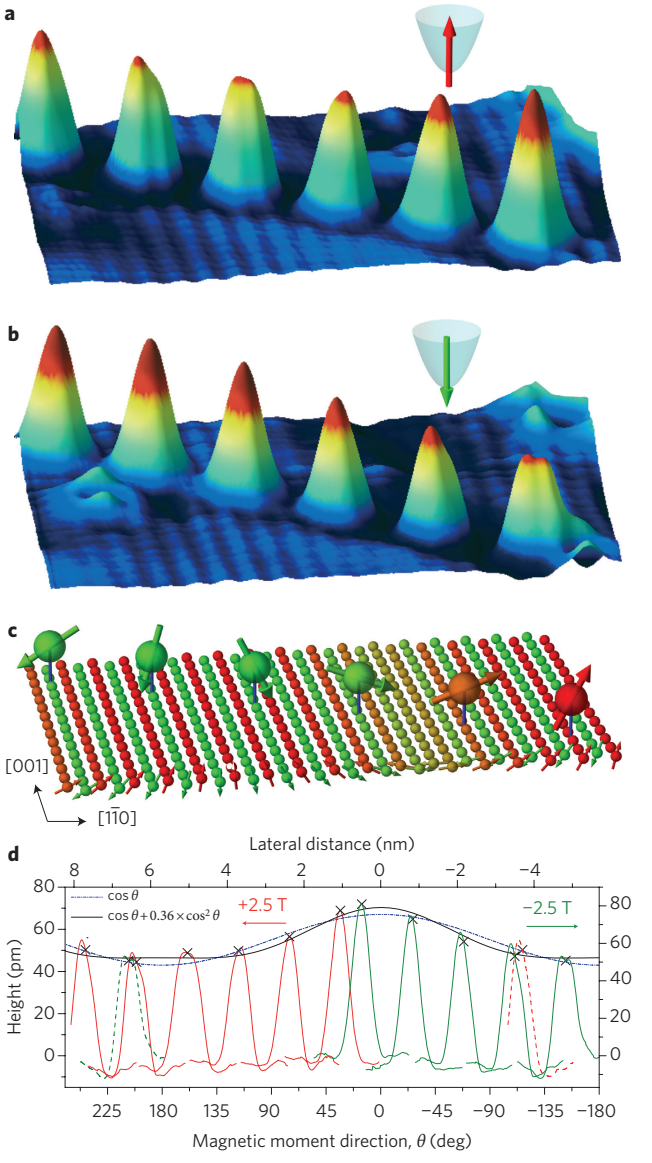

Figure 4 | Chain of cobalt atoms constructed by atom manipulation while maintaining spin resolution measured with an up and down magnetized tip. a,**b**, Perspective views of SP-STM images ($U = -10$ mV, $I = 2$ nA) taken with upwards (**a**) and downwards (**b**) pointing tip magnetization (see insets), thereby reversing the spin sensitivity. Raw data have been smoothed with a Gaussian to reduce noise. **c**, Atoms within the chain are equally spaced with a nominal angle of ~42° between adjacent cobalt moments. **d**, Line profiles across the cobalt atoms in **a** and **b** taken along the [1$\bar{1}$0] direction and positioned as a function of θ, determined from fits to the spin spiral. Different left and right axes are due to a slight tip change between measurements. The apparent height at the atomic centres (crosses) has been fitted with a cos θ (dot-dashed line) and the function $a_1\cos\theta + a_2\cos^2\theta$ (solid line).

Figure 3c and the corresponding line profiles across the centre of the cobalt atoms along [1$\bar{1}$0] in Fig. 3d reveal that in this example they appear asymmetric: the position of maximum height is shifted away from the atom centres. To investigate the origin of this effect systematically, we constructed a chain of equally spaced cobalt atoms (Fig. 4). The spin polarization of the tip is preserved throughout the atom manipulation process (see Supplementary Methods S5 and Movie), and thus the magnetic superstructure of the spin spiral could be used as a grid to precisely position the atoms. Figure 4a,b shows the change in topographic appearance of the atoms in the chain when the tip magnetization is reversed (see Methods). As illustrated in Fig. 4c, the cobalt atoms are separated by six atomic rows in the [1$\bar{1}$0] direction and four rows in the [001] direction, which results in a nominal angle of ~42° between adjacent cobalt moments, derived from the measured period of the spin spiral. The cobalt atoms in the chain display a gradual transition from a majority dominated appearance (rotational symmetry) to a minority dominated one (d_{xz} symmetry) via asymmetric states (Fig. 4a,b). Each angle θ of the cobalt moments with respect to the tip magnetization corresponds to a specific height and shape in the SP-STM measurement. Line profiles across the atomic centres along the [1$\bar{1}$0] direction are displayed in Fig. 4d, positioned as a function of the angle θ. Although the height at the atomic centres (crosses) roughly follows a cosine (dot-dashed line) profile, better agreement can be achieved with a higher-order correction, mixing 36% of $\cos^2\theta$ (solid line). Reasons for this might be the effect of spin–orbit coupling[16] onto the charge distribution or the constant-current measuring mode, because the cos θ in equation (1) is exact only at constant height.

The asymmetric shapes of cobalt atoms, which are observed in SP-STM images when their magnetic moments are non-collinear to the tip magnetization ($\theta \neq 0°, 180°$), cannot be explained based on electronic states with a single quantization axis. If both states, $n_S^{\uparrow}$ and $n_S^{\downarrow}$, are mirror symmetric (Fig. 2), this symmetry is preserved by equation (1) for any angle θ, in contrast to the experiment. The missing ingredient is the non-collinear magnetization of the manganese template underneath the cobalt atom, which is a vector field rotating ~173°

between adjacent atomic rows[9]. Because the local magnetization density above the cobalt atom, which extends approximately over three manganese rows, must connect smoothly to the one above the Mn/W(110) surface, it is also non-collinear; that is, $\theta(\mathbf{r})$ changes significantly within the extent of the cobalt states. Therefore, for a spin-polarized tip, the two sides of the cobalt states are not equivalent, and atoms with angles $+\theta$ and $-\theta$, as in Fig. 3c, can be distinguished. This means that although the height of the atoms allows a determination of the absolute value $|\theta|$, the degree of asymmetry provides information about the angle θ itself.

This work demonstrates not only direct access to the spin direction of individual atoms via differently shaped spin-polarized orbitals, but also the feasibility of performing atom manipulation with a spin-sensitive tip, thereby providing an approach for investigating bottom-up structures at an atomic level with spin sensitivity.

Methods

The experiments were conducted with a home-built STM at $T = 10$ K in ultrahigh vacuum[17]. The cobalt atoms were deposited *in situ* onto the magnetic template at $T < 20$ K to prevent diffusion. Magnetic tips were prepared by deposition of 30–40 atomic layers of iron onto a tungsten tip[10]. The spin-resolved measurements presented here were performed in magnetic fields of $|B| \geq 2$ T applied perpendicular to the sample surface, which aligns the tip magnetization, resulting in magnetic out-of-plane sensitivity (Fig. 1, $B = +2$ T; Figs 3,4a, $B = +2.5$ T; Fig. 4b, $B = -2.5$ T). The magnetic state of the manganese layer is unaffected by these low fields, because its spatially averaged magnetization is zero. Atom manipulation was performed by approaching the STM tip towards the atom and then moving the tip laterally at constant current (pulling mode)[11]. We found that the cobalt atoms could be moved reliably along ⟨111⟩ in-plane directions, that is, parallel to the close-packed manganese rows, using tunnel parameters of $U = 2$ mV and $I = 50$ nA (ref. 18). Image processing was carried out with WSxM (ref. 19).

Received 2 November 2009; accepted 4 March 2010; published online 25 April 2010

References

1. Gambardella, P. *et al*. Giant magnetic anisotropy of single cobalt atoms and nanoparticles. *Science* **300,** 1130–1133 (2003).
2. Meier, F., Zhou, L., Wiebe, J. & Wiesendanger, R. Revealing magnetic interactions from single-atom magnetization curves. *Science* **320,** 82–86 (2008).
3. Li, J., Schneider, W.-D., Berndt, R. & Delley, B. Kondo scattering observed at a single magnetic impurity. *Phys. Rev. Lett.* **80,** 2893–2896 (1998).
4. Madhavan, V., Chen, W., Jamneala, T., Crommie, M. F. & Wingreen, N. S. Tunneling into a single magnetic atom: spectroscopic evidence of the Kondo resonance. *Science* **280,** 567–569 (1998).
5. Heinrich, A. J., Gupta, J. A., Lutz, C. P. & Eigler, D. M. Single-atom spin-flip spectroscopy. *Science* **306,** 466–469 (2004).
6. Hirjibehedin, C. F., Lutz, C. P. & Heinrich, A. J. Spin coupling in engineered atomic structures. *Science* **312,** 1021–1024 (2006).
7. Yayon, Y., Brar, V. W., Senapati, L., Erwin, S. C. & Crommie, M. F. Observing spin polarization of individual magnetic adatoms. *Phys. Rev. Lett.* **99,** 067202 (2007).
8. Iacovita, C. *et al*. Visualizing the spin of individual cobalt–phthalocyanine molecules. *Phys. Rev. Lett.* **101,** 116602 (2008).
9. Bode, M. *et al*. Chiral magnetic order at surfaces driven by inversion asymmetry. *Nature* **447,** 190–193 (2007).
10. Heinze, S. *et al*. Real-space imaging of two-dimensional antiferromagnetism on the atomic scale. *Science* **288,** 1805–1808 (2000).
11. Eigler, D. M. & Schweizer, E. K. Positioning single atoms with a scanning tunnelling microscope. *Nature* **344,** 524–527 (1990).
12. Hohenberg, P. & Kohn, W. Inhomogeneous electron gas. *Phys. Rev.* **136,** B864–B871 (1964).
13. Zhang, Y. & Yang, W. Comment on 'generalized gradient approximation made simple'. *Phys. Rev. Lett.* **80,** 890 (1998).
14. Calculations were performed using the FLEUR code, http://www.flapw.de
15. Wortmann, D. *et al*. Resolving complex atomic-scale spin structures by spin-polarized scanning tunneling microscopy. *Phys. Rev. Lett.* **86,** 4132–4135 (2001).
16. Bode, M. *et al*. Magnetization-direction-dependent local electronic structure probed by scanning tunneling spectroscopy. *Phys. Rev. Lett.* **89,** 237205 (2002).
17. Pietzsch, O., Kubetzka, A., Haude, D., Bode, M. & Wiesendanger, R. A low-temperature ultrahigh vacuum scanning tunneling microscope with a split-coil magnet and a rotary motion stepper motor for high spatial resolution studies of surface magnetism. *Rev. Sci. Instrum.* **71,** 424–430 (2000).
18. Hla, S.-W., Braun, K.-F. & Rieder, K.-H. Single-atom manipulation mechanisms during a quantum corral construction. *Phys. Rev. B* **67,** 201402(R) (2003).
19. Horcas, I., Fernandez, R., Gomez-Rodriguez, J. M., Colchero, J., Gomez-Herrero, J. & Baro, A. M. WSXM: a software for scanning probe microscopy and a tool for nanotechnology. *Rev. Sci. Instrum.* **78,** 013705 (2007).

Acknowledgements

Financial support from the Deutsche Forschungsgemeinschaft (SFB668), the European Union ERC Advanced Grant FURORE, the Landesexzellenzcluster NANOSPINTRONICS, the Stifterverband für die Deutsche Wissenschaft, the Interdisciplinary Nanoscience Center Hamburg (INCH), the Marie Curie program (MEIF-CT-2006-039071) and the National Science Foundation program PIRE (OISE 0730257) is gratefully acknowledged. We appreciate valuable technical support from M. Langer and fruitful discussions with A. Khajetoorians and C. Lazo.

Author contributions

D.S. and A.K. provided the experimental concept and performed SP-STM. S.-W.H. and Y.Y. carried out atom manipulation, and M.M. and K.v.B. prepared the samples. P.F. and S.H. conducted DFT calculations. All authors discussed the results and prepared the manuscript.

Additional information

The authors declare no competing financial interests. Supplementary information accompanies this paper at www.nature.com/naturenanotechnology. Reprints and permission information is available online at http://npg.nature.com/reprintsandpermissions/. Correspondence and requests for materials should be addressed to A.K.